

# **Diagnosis of a Sick Building by the Wind Doctors**

Robert N. Meroney, David E. Neff and Cheng-Hsin Chang

*Department of Civil Engineering  
Colorado State University  
Fort Collins, 80523 USA*

Invited Plenary Session Paper for

The Second International Symposium on  
**Advances in Wind and Structures  
(AWAS'02)**

21-23 August 2002,  
Pusan Convention Center  
Pusan, Korea

## **Diagnosis of a Sick Building by the Wind Doctors**

\*Robert N. Meroney<sup>1</sup>, David E. Neff<sup>2</sup> and Cheng-Hsin Chang<sup>3</sup>

*Department of Civil Engineering, Colorado State University, Fort Collins, 80523 USA*

### **ABSTRACT**

A wind-sick building at the Denver Federal Center, Colorado, USA was examined by the CSU Wind Doctors using MRI (Measurement Research Investigation) and CATscan (CFD Aerodynamic Testing) diagnostic techniques to determine a proper course of treatment to alleviate severe skin and breathing problems. The evaluation determined that the building's sickness was due to severe extreme wind exposure. A prescription was written to provide protection through constructive plastic surgery on the face of the building and the insertion of supportive landscaping orthotics around the foot of the structure. The prognosis is for significantly improved quality of life, but problems will persist even if various landscaping improvements mature.

### **INTRODUCTION**

A significant characteristic of modern building design is lighter cladding and more flexible frames. These features produce an increased vulnerability of glass and cladding to wind damage and result in larger deflections of the building frame. In addition, increased use of pedestrian plazas at the base of the buildings has brought about a need to consider the effects of wind and gustiness in the design of these areas. Tall structures have historically produced unpleasant wind and turbulence conditions at their bases. The intensity and frequency of objectionable winds in pedestrian areas is influenced both by the structure shape and by the shape and position of adjacent structures. The two primary design methods available today to evaluate wind effects on tall structures are physical modeling (wind or water tunnels) and computational fluid dynamics (cfD). A case study is considered where both methods are compared to consider their advantages, disadvantages, and evidence for agreement in results.

---

<sup>1</sup>Professor, Ph.D.    <sup>2</sup>Senior Research Scientist, Ph.D.    <sup>3</sup>Research Scientist, Ph.D.

## DIAGNOSTIC METHODOLOGIES

MRI (Measurement Research Investigation) techniques have been developed for wind-tunnel modeling of structures which allow the prediction of wind pressures on cladding and windows, overall structural loading, and also wind velocities and gusts in pedestrian areas adjacent to the building. Information on sidewalk level gustiness allows plaza areas to be protected by design changes before (or after) the structure is constructed. Accurate knowledge of the intensity and distribution of the pressures on the structure permits adequate but economical selection of cladding strength to meet selected maximum design winds and overall wind loads for the design of the frame for flexural control. A detailed discussion of the similarity requirements and their wind-tunnel implementation can be found in Isyumov (1999). In general, the requirements are that the model and prototype be geometrically similar, that the approach mean velocity at the building site have a vertical profile shape similar to the full-scale flow, that the turbulence characteristics of the flows be similar, and that the Reynolds number for the model building be greater than a critical value. These criteria are satisfied by constructing a scale model of the structure and its surroundings and performing the wind tests in a wind tunnel specifically designed to model atmospheric boundary-layer flows.

Simulation of flow and forces around buildings using CATscan (CFD Aerodynamics Testing) requires consideration of many of the same concerns and constraints as physical modeling. One must assure equivalence of inlet and boundary conditions, geometric similarity of the model, consideration of spatial resolution of any numerical grid, and appropriateness of the computational turbulence model. Various authors have considered these topics at length in recent specialty conferences, (Murakami, 1992; Meroney and Bienkiewicz, 1996; Baker, 2000).

## THE BUILDING PATIENT AND ITS SYMPTOMS

The wind-engineering study is performed for a specific patient, Building 67 of the Denver Federal Center, Denver, CO, USA (Neff, *et al.*, 2001). The patient was born in 1967 in Denver, Colorado to its parents the Federal Bureau of Reclamation. It is now 35 years old, 210 feet tall, and is employed but disabled. Its wind related medical symptoms include skin defoliation (repeated window breakage, mullion and cladding failure) and breathing problems (hard to open doors, dangerous and gusty plaza and high winds in the parking area). The building guardians, the Federal General Services Administration, desire to cure the patient and return it to full health and normal activity. The CSU Wind Doctors were consulted, and it was concluded that diagnostic testing using MRI and CAT scan techniques were appropriate. In addition it was considered appropriate to evaluate the severity of the patient's local wind exposure with an Extreme Wind Analysis (EWA).



**Fig. 1.** Building 67, Denver Federal Center, CO

## EXTREME WIND ANALYSIS (EWA)

Building 67 of the Denver Federal Center lies west of US Interstate Highway 25 and south of 6th Avenue in Denver. This region near the foothills of the Rocky Mountain is in a Special Wind Zone on the ASCE 7-98 extreme wind map; hence, the recommendation is to use local climatological data to specify the 50-year return period 3-second gust conditions (ASCE, 1998). Weather data from DIA or Stapleton Airports near Denver are not suitable because the anemometers are located to the east away from the foothills. Unfortunately, data for the foothills region is extremely limited. No regular data sets are archived by the US National Climatological Data Center, the Rocky Mountain Regional Climatological Center or the Colorado Climate Center.

Individual wind speeds have been measured during short measurement programs along the foothills, which are quite large. The National Center for Atmospheric Research had an automatic weather station running on the mesa above Boulder for many years. During a windstorm in January 1972, they recorded a maximum gust speed of 236 km/hr (147 mph), and during another storm in January 1982 NCAR recorded 220 km/hr (137 mph). The anemometer registered a continuous trace near 169 km/hr (105 mph), with gusts near 201 km/hr (125 mph) for at least an hour about midnight during the 1982 storm. A shorter period (~10 years, 1969-1978) digital record of extreme wind speeds was finally acquired from the NOAA Forecast Systems Laboratory, Boulder. The gust data were taken by an anemometer mounted on the central building (Number 1) of the U.S. Department of Commerce Building on the west side of Broadway at 27th Way, Boulder, CO. The anemometer was a 3-cup type with a large distance constant. The anemometer was mounted at a height of about 10 m above ground at approximately 1658 m (5440 ft) MSL. The data was continuously recorded via a strip-chart recorder, and peak gusts were read and entered by hand in a tabular form every 3 hours. A zero was entered if the peak gust was less than 37 km/hr (20 knots). The data was digitized in 1990 by transcribing from the tabular sheets. The gusts recorded during this period of ten years may be on the high side since it spans one of the windiest periods of modern Boulder history.

The NOAA Forecast Systems Laboratory data described above were sorted, zeros and no-data days were removed, and a Gumble analysis was applied to the sequence to determine the probability distribution for extreme winds. The result was a value for 3-second gust speed of 177 km/hr (110 mph) for a 50-year return period. A second analysis of the same data was applied as suggested by the text by Simiu and Scanlan (1996) based on mean and standard deviation of the data set that predicated a 171 km/hr (106 mph) wind speed for a 50-year return period. Both of these values are substantially larger than the 145 km/hr (90 mph) value suggested by the ASCE 7-98 code for regions east of Interstate 25.

## MEASUREMENT RESEARCH INVESTIGATION (MRI)

The patient building group was modeled at a scale of 1:240 in the Environmental Wind Tunnel at Colorado State University. Surrounding buildings and terrain were incorporated out to a 825 m radius from the complex. Structures within the modeled region were made from Styrofoam and cut to the individual building geometries. Significant terrain features were also included. The model was mounted on a turntable near the downwind end of the Environmental Wind Tunnel test section. The region upstream from the modeled area was covered with a generic cubical roughness placed on the floor of the wind tunnel. Spires were installed at the



Fig. 2. Model (1:240) scale in Environmental Wind Tunnel, WEFL, Colorado State

test-section entrance to provide a thicker boundary layer than would otherwise be available. The distribution of the roughness cubes and the spires in the roughened area was designed to provide a boundary-layer thickness of approximately 1.5 m, surface roughness of 0.18 m and a velocity profile power-law exponent of 0.2 similar to that expected to occur in the region approaching the modeled area.

The model patient building was constructed of plastic and fastened together with metal screws. Significant variations in the building surface, such as mullions, were

machined into the plastic surface. Pressure taps (1.6 mm diameter) were drilled normal to the exterior vertical surfaces in rows at several or more elevations between the bottom and the top of the building. Pressure tap locations were chosen so that the entire surface of the building could be investigated for pressure loading and at the same time permit critical examination of areas where experience has shown that maximum wind effects may be expected to occur.

The test model, equipped with many pressure taps (376 for this study), was exposed to an appropriately modeled atmospheric wind in the wind tunnel and the fluctuating pressure at each tap measured electronically. The individual pressure taps were connected to four forty-eight-port pressure-switching valves mounted near the model via 2 mm I.D. plastic tubing. The four pneumatic outputs from these valves were connected to the pressure side of four differential pressure transducers via short lengths of plastic tubing. Reference pressures were obtained by connecting the reference sides of the four transducers to the static side of a pitot-static probe mounted in the wind tunnel free stream above the model building. In this way, the transducer measured the instantaneous difference between the local pressures on the surface of the building and the static pressure in the free stream above the model. Honeywell Microswitch pressure transducers with a  $\pm 1200$  pascal range were used. A computer controlled a stepper motor, which changed the position of all four multi-port pressure valves simultaneously. The model and the modeled area were rotated to the next wind angle and another set of data recorded for each pressure tap.

Based on a set of visualization (smoke) tests and on a knowledge of heavy pedestrian use areas, several locations were chosen at the base of the building to determine the wind comfort levels. Hot-film anemometers made mean velocity and turbulence intensity measurements 2 meters (prototype) above the surface at several locations near the building for different wind directions (See Fig. 3). The surface measurements are indicative of the wind environment to which a pedestrian at the measurement location would be subjected. The locations were chosen to determine the degree of pedestrian comfort or discomfort at the building corners where relatively severe conditions are frequently found, near building entrances and on adjacent sidewalks where pedestrian traffic is heavy. Pedestrian wind speed data were obtained for six possible shelter configurations, designated as configuration A through F for five wind directions

(N, NNW, NW, WNW,). The shelters included various combinations of 1.25 and 2.5 m high fences, 4.6-5.5 m high tree rows, 9.1-10.7 m high tree rows and building canopies.

### CFD AERODYNAMIC TESTING (CATscan)

Various configurations of Building 67 were also considered by numerically modeling the patient building and flow field using the commercial code Fluent 5.5. Computational grids were prepared for various wind angles using the preprocessor code Gambit. A computational domain 356 m long, 365 m wide and 183 m high was divided into 328,000 tetrahedral cells. Alternative turbulence models were considered to check sensitivity of the results to model selection including kappa-epsilon, RNG-kappa-epsilon, and large-eddy simulation techniques. Only model orientations normal to the north face ( $330^\circ$ ) and at 45 degrees to the north and west faces ( $285^\circ$ ) were considered; however, base configurations with no pedestrian wind mitigation and the inclusion of plaza level barriers were examined. Since only steady-state approach flows with appropriate velocity and turbulence profiles were considered, only average surface pressure coefficients over the building were calculated.

During the three-dimensional CFD investigation of Building 67 only a smooth faced virtual structure was considered (without the window embrasures and sun-shades). However, a separate two-dimensional CFD investigation of the building cross-section was completed for both smooth models and models including window embrasures. The results indicated that whereas the additional mullions do cause local pressure variations, the trends are equivalent and deviations are not major; hence, a smooth three-dimensional virtual model was deemed adequate for this study.

### WIND DOCTOR'S REPORT

#### Extreme Wind Analysis

The Gumble analysis discussed previously suggests a 3-second gust speed of 177 km/hr (110 mph) for a 50 year return period. The statistical analysis based on means and standard deviation from Simiu & Scanlan (1996) predicts a 3-second gust speed of 171 km/hr (106 mph) for a 50-year return period. The actual return period for 145 km/hr (90 mph) winds is about 3.5 years and for 129 km/hr (80 mph) winds is 1 year! The identified differences imply that the facade for Building 67 should be designed for forces ~38-50% times greater than those predicted by the code in place at the time the building was born.

#### MRI Results

Wind loads The largest peak and mean pressure coefficients measured on the building for each pressure tap location for all wind orientations were tabulated. These tables also included the corresponding loads in pounds per square foot (psf) measured on the building for each pressure tap location. The largest suction pressures obtained on the building ranged up to -61 psf (-2.9 k Pascals outward acting) and were located near the corners on the tower and adjacent to the roof. The largest positive pressures obtained on the building ranged up to +47 psf (+2.3 k Pascals inward acting) and were located on the upper building floors. Most of the area of the building had peak negative pressures less than -45 psf (-2.2 k Pascals) with higher pressures restricted to limited areas. Typical peak positive pressures were ~40 psf (~1.9 k Pascals) (See Fig. 4, 5, 6 and 7).

Pedestrian level winds The largest mean velocities were measured at the northwest and southwest corners of Building 67 (locations 13, 14, 19, 21). The values were up to 60-70 percent of the gradient height (335m) wind speed,  $U_g$ . The mean wind speed directly in front of the entrance doors (locations 15-16, 20) had low values of 10-30 percent of  $U_g$ . Most of the outlying points had maximum mean wind speeds of 40-50 percent of  $U_g$ . These wind speeds can be compared to 40 to 45 percent, which might be found in an open-country environment. The largest gust velocities, represented by the mean plus 3 rms were measured at location 13 with values of ~100 to 110 percent of  $U_g$ . These values are high when compared with values of 80 to 90 percent in an open-country environment.

Comparisons between the different shelter configurations and that of the existing configuration show that none of the tested configurations improved the overall wind environment. At some locations, the fencing increased the wind outflow in front of the building. It is suggested that local wind barriers be placed near the corners of Building 67 if these areas are envisioned to be heavily used by pedestrians. Another potential improvement might be the development of trees and buildings on a substantial fetch upwind of Building 67. The placement of just a small row of trees was demonstrated to be ineffective in the present study.

### CATscan Results

Wind loads CFD analysis were completed for winds approaching perpendicular to the north building face (NNW) and at an angle of 45degrees from the nominal WNW directions. Average surface pressure coefficients over these faces varied from 0.41 to -0.89 (+14.5 to -31.4 PSF) for NNW winds with maximums at the central face of the north wall. Surface pressure coefficients over the upwind faces for the WNW winds varied from 0.15 to -0.13 (+5.3 to - 5.0 PSF) with maximums occurring on the windward corner and highest suction pressures occurred along the trailing edges of the downwind wall surfaces (See Fig. 8 and 9).

Pedestrian level winds CFD analysis replicated the physical models conclusion that none of the proposed sheltering options significantly improved wind fields around the building or over the plaza. The addition of 2.5 m walls did change the flow patterns, for they merely displaced wind around on the plaza but did not significantly diminish their magnitudes. Wind patterns and vectors were similar.

### MRI and CATscan Comparisons

Fig. 10, 11 and 12 compare pressure coefficients for NNW ( $330^\circ$ ) winds on the northern and western faces of Building 67 as predicted by the MRI and CATscan investigations. The MRI fluid model results exhibit variability associated with the location of the pressure taps within the window embrasures on the building faces. The CATscan pressure profiles are relatively smooth since such surface irregularities were absent on the numerical virtual building faces. Nonetheless, the two data sets have similar magnitudes and show similar trends. On the north face pressure coefficients are maximum near building center and diminish toward the corners. The pressures also tend to increase as one moves from lower to upper building floors. On the west face high suction pressures occur just downwind of the windward corner, and pressure coefficients steadily increase toward the trailing building edge.

## PROGNOSIS

Pressure coefficients of several types were calculated for each physical model pressure tap. Integration of test data with wind data resulted in prediction of peak local wind pressures for design of glass or cladding. Pressure contours were drawn on the developed building surfaces showing the intensity and distribution of peak wind loads on the building. Examination of winds at ground level for pedestrian comfort identified several alternative windbreak and landscaping scenarios that only slightly reduce pedestrian winds.

- Window breakage will decline
- Facade damage and falling debris will cease
- Pedestrian comfort problems will remain

## CONCLUSIONS CONCERNING MRI and CATscan COMPARISONS

Similar pressure and wind flow presentations were produced by the physical model (MRI) measurements and cfd (CATscan) calculations. Initial conclusions are:

- The general character of flow about the building produced by the two modeling alternatives is very similar. Regions of flow acceleration, separation, reattachment, and evidence for rooftop and ground level vortices are evident.
- Mean pressure coefficients calculated by the two modeling alternatives are very similar. Regions of positive pressure and negative suction are coincident in both models.
- Landscaping and architectural alternatives considered during the two model alternatives produced similar conclusions concerning useful modifications to the plaza area.

## REFERENCES

- American Society of Civil Engineers (1998) , *Minimum Design Loads for Buildings and Other Structures*, ASCE 7-98.
- Isumov, N., editor (1999), *Wind Tunnel Studies of Buildings and Structures*, ASCE Manuals and Reports on Engineering Practice No. 67, American Society of Civil Engineering, ISBN: 0\_7844\_0319\_8, 232 pp.
- Murakami, S., editor (1993), *Proceedings of 1<sup>st</sup> Int. Symposium on Computational Wind Engineering*, U. of Tokyo, Japan, 21-24 August 1992, also *Jrnl. of Wind Eng. and Ind. Aero.*, Vol. 46-47, 1993.
- Meroney, R.N and Bienkiewicz, B. editors (1997), *Proceedings of 2<sup>nd</sup> Int. Symposium on Computational Wind Engineering (CWE96)*, Colorado State University, Fort Collins, 4-8 August 1996, also *Computational Wind Engineering 2*, Elsevier, Amsterdam, 1997.
- Neff, D. E., Meroney, R.N., Chang, C.H. and Pradato, R. (2001), *Wind Tunnel Study of Cladding Wind Loading and Pedestrian Wind Environment for Building 67*, Denver Federal Center, Report to Oz Architecture, Denver, CO, 65 pp.
- Baker, C., editor (2000), *Proceedings of 3<sup>rd</sup> Int. Symposium on Computational Wind Engineering (CWE2000)*, Univ. of Birmingham, UK, 4-7 September 2000.
- Simiu, E. and Scanlan R. (1996), *Wind Effects on Structures: Fundamentals and Applications to Design*, 3<sup>rd</sup> edition, John Wiley & Sons, New York, 688 pp.

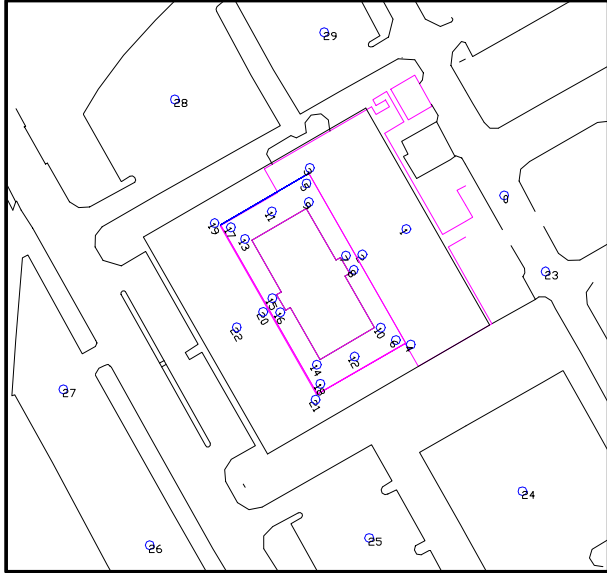


**Fig. 3a** Pedestrian Velocity Measurement Locations

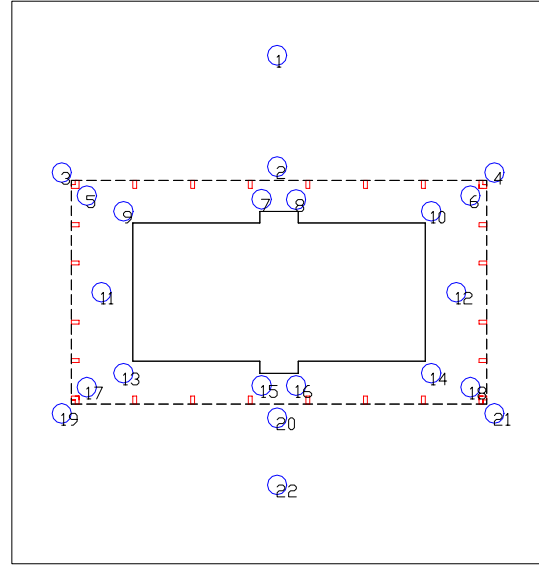


**Fig. 3b** Plaza Pedestrian Velocity Measurement Locations

**FACE #1 (North Side) - Largest PSF Minimums**

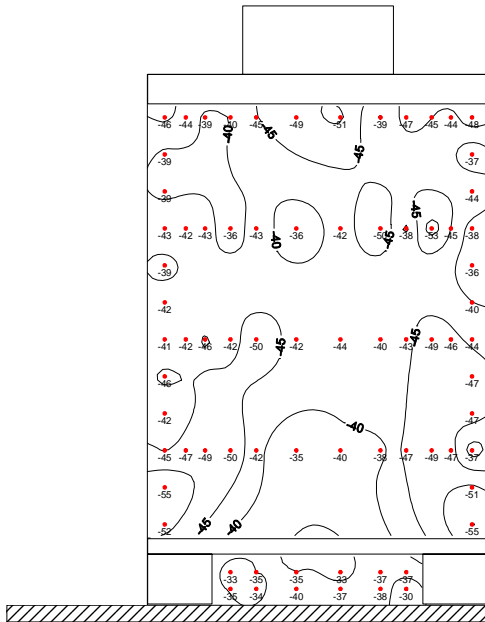


**Fig. 4** Largest PSF Minimums North Face

**FACE #1 (North Side) - Largest PSF Maximums**

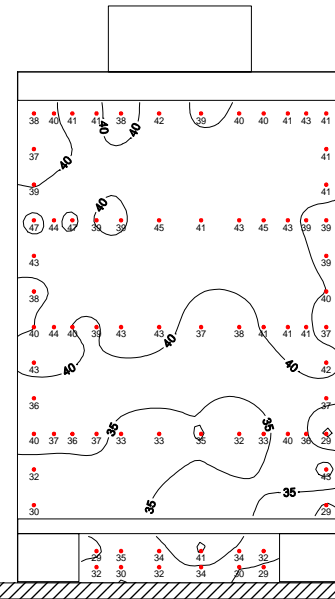


**Fig. 5** Largest PSF Maximums North Face

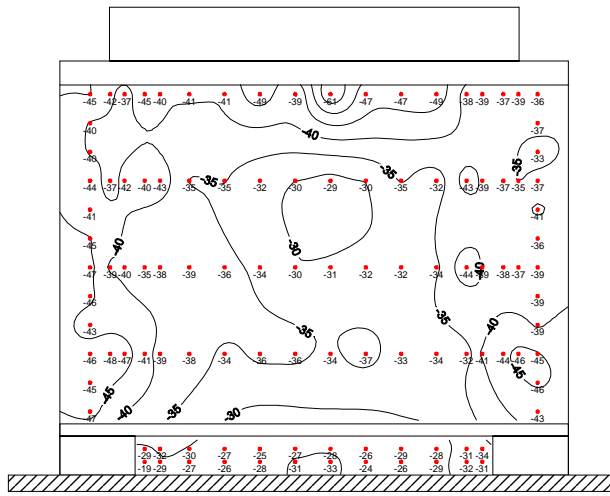


Fig. 6 Largest PSF Minimums West Face

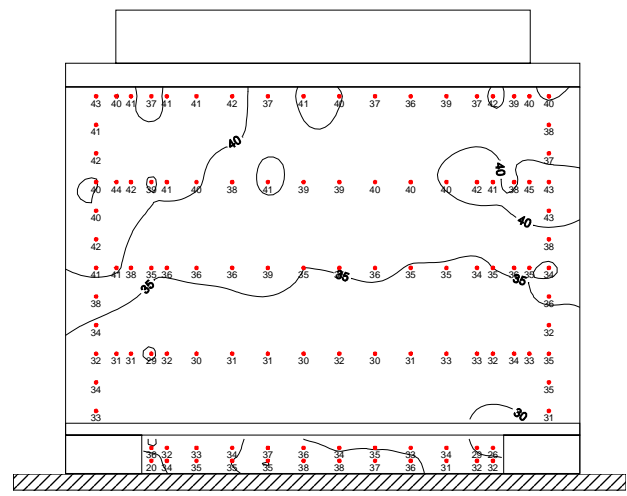


Fig. 7 Largest PSF Maximums West Face

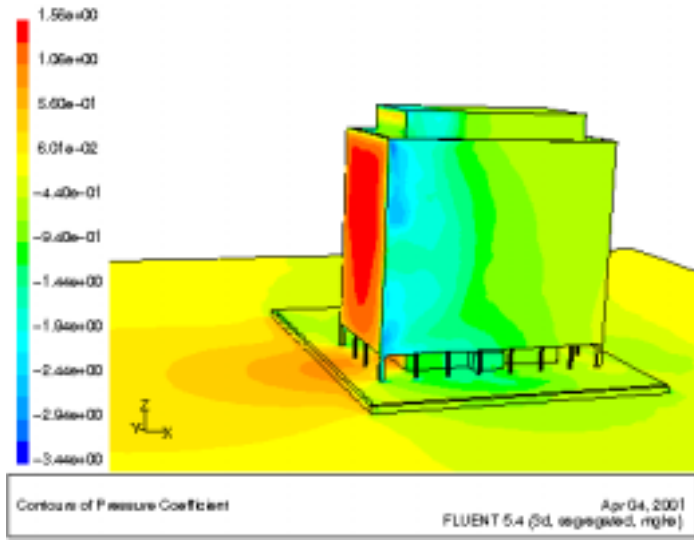
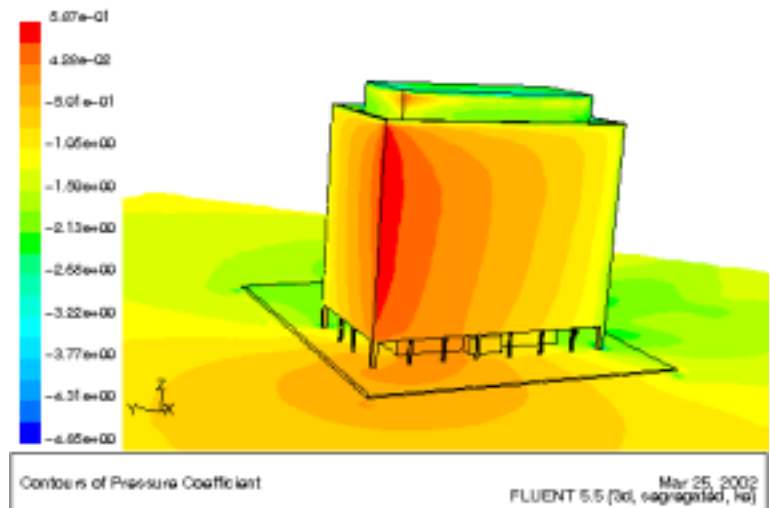
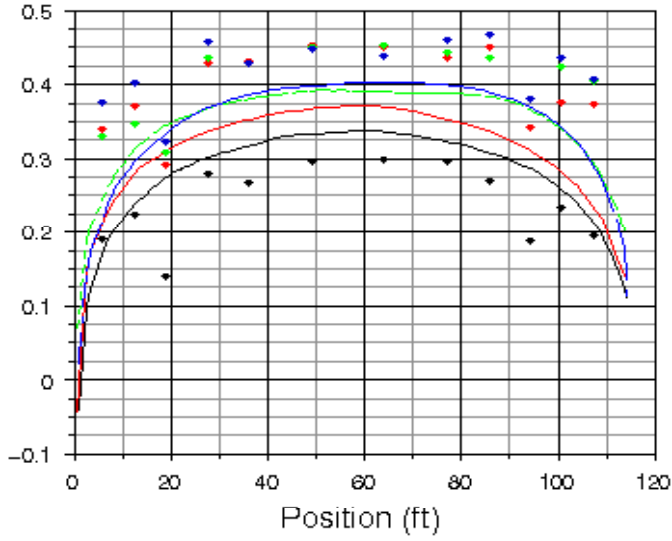


Fig. 8 Average Pressure Coefficients for NNW Winds

Fig. 9 Average Pressure Coefficients for WNW Winds





**Fig. 10** MRI and CATscan Pressure Coefficient Comparison, North Face, NNW winds

**Fig. 11** MRI and CATscan Pressure Coefficient Comparison, West Face, NNW winds

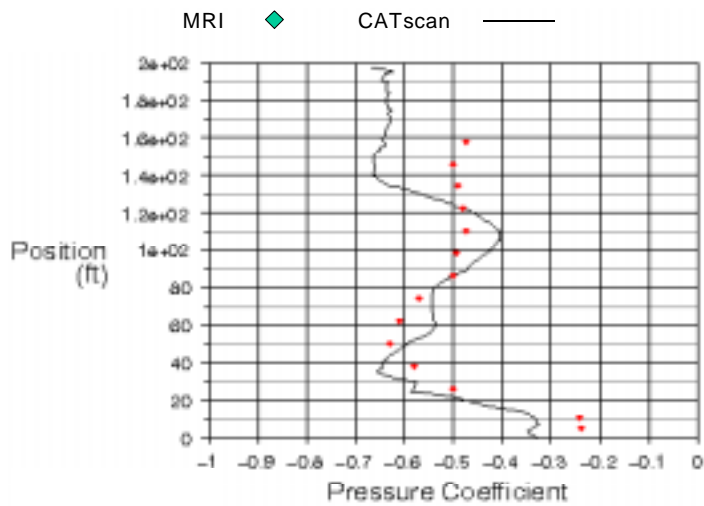
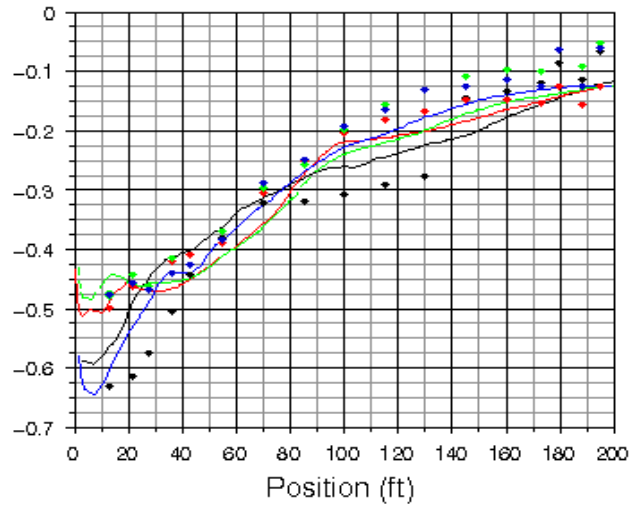


**Fig. 12** MRI and CATscan Pressure Coefficient Comparison, West Face, NNW winds along vertical line along upwind edge